



HAL
open science

Phosphate dynamics in an urban sewer: A case study of Nancy, France

J. Houhou, B.S. Lartiges, A. Hofmann, G. Frappier, J. Ghanbaja, A. Temgoua

► **To cite this version:**

J. Houhou, B.S. Lartiges, A. Hofmann, G. Frappier, J. Ghanbaja, et al.. Phosphate dynamics in an urban sewer: A case study of Nancy, France. *Water Research*, 2009, 43 (4), pp.1088-1100. <10.1016/j.watres.2008.11.052>. <hal-02264644>

HAL Id: hal-02264644

<https://hal.science/hal-02264644v1>

Submitted on 7 Aug 2019

HAL is a multi-disciplinary open access archive for the deposit and dissemination of scientific research documents, whether they are published or not. The documents may come from teaching and research institutions in France or abroad, or from public or private research centers.

L'archive ouverte pluridisciplinaire **HAL**, est destinée au dépôt et à la diffusion de documents scientifiques de niveau recherche, publiés ou non, émanant des établissements d'enseignement et de recherche français ou étrangers, des laboratoires publics ou privés.



HAL Authorization

PHOSPHATE DYNAMICS IN AN URBAN SEWER

J. Houhou¹, B.S. Lartiges^{1*}, A. Hofmann², G. Frappier¹, J. Ghanbaja³, A. Temgoua¹

¹ Nancy University – LEM-ENSG/INPL-CNRS, Pôle de l'Eau 15 Avenue du Charmois
- BP 40 54501 Vandœuvre Cedex, France

² Lille University-Géosystèmes 8157 UMR-CNRS, Cité scientifique, 59655 Villeneuve
d'Ascq, France

³ Nancy University – Service Commun de Microscopie - BP 239 - 54 500 Vandœuvre
Cedex, France

E-mail: bruno.lartiges@get.omp.eu

(*) To whom correspondence should be addressed

ABSTRACT

The nature of phosphate phases present in suspended matter, biofilm, and sediment of Greater Nancy sewer system, was investigated over a period of two years. The phosphate speciation was determined by two approaches: a direct identification of phosphorus mineral phases was conducted by Transmission Electron Microscopy (TEM) coupled with Energy Dispersive X-ray Spectroscopy (EDXS), whereas a chemical extraction of samples provided an estimate of phosphorus pools defined by the fractionation scheme. Quantitative analysis of 1340 individual particles allowed to draw a picture of phosphate species distributions along the sewer system and over time. Amorphous Ca-phosphates (brushite, whitlockite, octacalcium phosphate, Mg-brushite, hydroxyapatite and carboxapatite) are ubiquitous although brushite dominated upstream, and octacalcium phosphate and apatite prevailed downstream and in sediments. Al-Ca-phosphate minerals such as foggite, bearthite, gatumbaite, and crandallite appeared downstream and in biofilms. Changes in Ca-phosphate phase distribution were related to phase transformations from brushite to hydroxyapatite that were shown to be kinetically driven. The restriction of Al-Ca-phosphates to downstream of the sewer system was most probably related to the lower pHs measured at these sites. The pH dependency was confirmed by stability calculations. TEM examination of chemical extraction residues revealed the presence of neoformed Al-Ca-phosphate species that invalidate the fractionation scheme. On the other hand, it confirmed that phosphate phases may undergo significant geochemical changes over a short time scale.

Keywords: Phosphate, chemical extraction, sewer system, TEM-EDXS, brushite, hydroxyapatite, foggite, crandallite.

INTRODUCTION

Traditionally designed to be a simple drainage system for wastewater, the sewer network is now recognized as a true biophysicochemical reactor, or in other terms, as an integrated part of the wastewater treatment system (Hvitved-Jacobsen et al. 1995; Warith et al. 1998). Hydrogen sulfide production (Yongsiri et al. 2004; Zhang et al. 2008) and methane emission (Guisasola et al. 2008) readily illustrate such a role. In addition, the nature of organic matter contained in sewage has been shown to evolve during transport (Raunkjaer et al. 1994; Chen et al. 2001).

Phosphorus, mainly present in sewage as orthophosphate (Butler et al. 1995), is also likely to participate in the dynamics of such a reactor. Indeed, orthophosphate is known to quickly interact - uptake and release - with a wide variety of natural surfaces (Froelich 1988; House 2003), the composition of phosphate minerals precipitated from supersaturated solutions is kinetically controlled (Nancollas and Tomazic 1974), and as an essential nutrient, phosphate can be utilized by microorganisms (Mulkerrins et al. 2004). Such complex dynamics have for instance been evidenced in urine-collecting systems (Udert et al., 2003a).

The main objective of this study was to describe the fate of orthophosphate along the sewer system. This involved the speciation of phosphate mineral species encountered in suspended matter, biofilms, and sediments of the sewer, by electron microscopy combined with energy-dispersive X-ray spectrometry (EDXS). Such a technique provides a direct identification of phosphate carriers at the nanoscale (El Samrani et al. 2004). A chemical extraction was also conducted to assess the various pools of phosphorus, despite the fact that these extractions can lead to erroneous results due to re-adsorption or re-precipitation phenomena.

EXPERIMENTAL SECTION

Study area. Samples were collected from the sewer network of Greater Nancy urban community. Nancy, a city of about 270 000 inhabitants located in north-eastern France, lies on both banks of Meurthe river with a total catchment area of 193 Km² (144 km² on left bank). The sewage collecting system comprises 950 km of pipes, 250 km of them man-entry sewer (pipe diameter \geq 1.2 m). As Nancy is established in a hill basin with hills dominating the Meurthe valley by about 200 m, the slope of the gravity sewer pipe may reach 5%. The central core of Nancy urban community is served by a combined sewer, whereas the

peripheral areas are drained by separate systems. 25 detention basins (180 000 m³ storage capacity) have been constructed to limit discharges from combined sewer overflows in the Meurthe river.

As illustrated in figure 1, three sewer sections, each with 5 sampling sites from upstream to downstream of the sewer network, were selected to represent the various land uses in the urban community (residential, commercial, industrial, high school, and hospital). Table 1 provides a summary of sampling sites characteristics. On a general basis, the upstream sampling site only receives domestic wastewater from a separated sewer, the following sampling site is impacted either by hospital or industrial wastewaters, whereas the downstream sampling sites mainly convey sewage from high density residential areas and small businesses through a combined sewer.

Sampling and chemical analyses. Eight sampling campaigns were conducted in dry weather conditions between November 2004 and October 2006. Grab-samples of sewage, and whenever possible biofilms and sediments, were collected from the sewer. Various categories of sewer sediment have been described in the literature: according to Crabtree (1989), the collected sediments correspond to type A coarse granular deposits. Sewage characteristics such as temperature, pH, conductivity, dissolved oxygen concentration, redox potential (WTW, Multiline F/SET) and turbidity (Hach 2100P), were measured immediately upon sampling. Part of the sewage was filtered on site through a pre-washed 0.22 µm pore size cellulose-acetate membrane (Chromafil[®] CA-20/25) and split into three aliquots for analyses of metals, anions, and dissolved organic carbon (DOC). The filtrates were stored at 4°C in 65 mL polyethylene or glass bottles until analysis. As such on-site sample preparation usually exceeded the mean transit time of sewage between two consecutive sampling sites (cf. Table 1), it was not possible to follow the evolution of the same body of sewage within the sewer network. The purpose of two 24h campaigns was then to investigate the variations in wastewater characteristics at a given sampling site as a function of time.

About 20 L of sewage were brought back to the laboratory in polyethylene jerrycans, and processed within four hours of sampling. After gentle end-over-end mixing of the jerrycans, the sewage was centrifuged in 1L polyethylene bottles at 15000 g for 30 min (Sorvall[®] Evolution RC). Total Suspended Solids (TSS) mass was determined by drying an aliquote of centrifuged sewage at 105°C for 12 hours, and Volatile Solids (VS) mass was obtained by further heating the same samples at 550°C for 4 hours. All samples were analysed

in duplicate. The sediments were sieved at 2 mm, 250 μm , and 50 μm , and the fractions collected were freeze-dried.

Table 2 summarizes the main physico-chemical characteristics of sewage collected during the eight sampling campaigns. DOC was measured with a Dohrman 190 analyzer. Phosphate, nitrate, and sulfate anions were determined by ion chromatography using a Dionex ICS-3000 (AS9-HC column). The lower detection limits were 50 ppb for PO_4 and 20 ppb for the other anions. Total soluble P, Ca, Al, and Fe, were obtained using a Jobin-Yvon JY70 ICP-AES. For total contents of these elements in the freeze-dried solid fractions, a 200 mg aliquot was first melted with 600 mg LiBO_3 in a Pt-Au crucible, and then dissolved with 1N HNO_3 . The resulting solution was analyzed by ICP-AES (Carignan et al. 2001).

Mineral phosphate speciation. Direct speciation of phosphate phases was mainly obtained by Transmission Electron Microscopy (TEM) combined with energy-dispersive X-ray spectrometry (EDXS). EDXS yields an elemental analysis of individual particles from freeze-dried solids. Stoichiometric ratios can be calculated and compared with known mineralogical compositions. Electron diffraction patterns provided by TEM, characterising the crystal structure of particles, can also be used for identification.. In this study, transmission electron microscopy observations were carried out with a Philips CM20 TEM (200 kV) coupled with an EDAX energy dispersive X-ray spectrometer. The freeze-dried powder was re-suspended in 2 mL ethanol under ultrasonication, and a drop of suspension was evaporated on a carbon-coated copper grid (EuroMEDEX Mesh200-Car#CF200CU) placed on filter paper. A spot size of about 70 nm and a counting time of 40 seconds were used to record EDX spectra. EDX calibration standards were run to obtain quantitative analyses of major and trace elements with a detection limit of about 100 ppm. In addition, a few samples were examined with a S-2500 Hitachi scanning electron microscope equipped with a Kevex 4850 EDX. In that case, freeze-dried powders were sprinkled onto 2 cm^2 plates and carbon coated. The SEM microscope was generally operated with a beam current of 3 pA and an accelerating voltage of 20 kV (analysed microvolume of about 6 μm^3).

An exploratory parallel extraction procedure was carried out to provide a chemical partitioning of phosphorus among various chemical forms. The extraction scheme originally developed for activated sludge by Moreau (1997), is summarized in Table 3. It allows to discriminate loosely sorbed P [L-P], inorganic P associated with aluminum [Al-P], inorganic P bonded to carbonates [Ca-P], inorganic P associated with reducible forms of Fe ([Fe-P], and P bonded to organic matter [OM-P]. Each sample was extracted in triplicate: 100 mg of

freeze-dried material (suspended matter, biofilm, or sediment) was treated with the reactant for a given time (Table 3). The extracts were centrifuged for 15 minutes at 4000 RPM (1613 g) and the supernatants were filtered with 0.22 μm pore size. Phosphate concentrations were determined by conventional molybdate colorimetry (Murphy and Riley 1962) on the supernatant solutions. To avoid any interference from fluoride ion during P determination, 5 mL of boric acid 0.5 M was added to supernatants from Al-P extractions (Chang and Jackson, 1957). In order to control the colorimetric procedure, phosphorus contained in extracts of labile P, aluminum and calcium bound fractions, was also analyzed by ICP-AES. The extraction residues were rinsed with 30 mL NaCl 0.3 M (20 min agitation), and centrifuged at 4000 rotations/min for 15 min. Samples were then rinsed with ultra pure water (18.5 m Ω - MilliQ-plus), again centrifuged and finally freeze-dried. The dry residues were examined by TEM-EDXS to check the selectivity and specificity of various extractants.

RESULTS

Phosphate content in sewage, biofilms and sewer sediments. The average concentrations and the ranges in soluble phosphorus, orthophosphate, and total solid phosphorus in suspended matter and sediment, are compiled in Table 4. Total soluble phosphorus varied considerably between 1.32 and 13.35 mg/L with an average concentration of 7.11 mg/L. The highest P levels were obtained in areas served by a separate sewer system, whereas the lowest P concentrations were observed at night in a sewer section characterized by a high influx of groundwater (Houhou et al., in preparation). All P values fall within the range of dissolved P concentrations typically reported for sewer systems (Jolley et al. 1998; Halliwell et al. 2001; Tchobanoglous et al. 2003). A plot of orthophosphate concentration versus total soluble P (Figure 2) indicated that orthophosphate largely dominated the dissolved P component in most samples, which is again in accordance with previous studies (Butler et al. 1995; Jolley et al. 1998).

About 20% of the total P content in sewage was in particulate form. This corresponds to a particulate phosphorus load in the 4.34-13.55 mg P/g range with an average value of 6.8 mg/g (Table 4). The average phosphorus content in sediments ranges from 0.9-7.5 mg/g, the < 50 μm sediment fraction showing the highest P concentration. Similar values have been reported for urban freshwater sediments (Taylor and Boulton 2007), and fluvial sediments impacted by sewage discharges (Owens and Walling 2002).

Using the average daily water use for France of 137 L, the average concentration of total P in sewage (10.13 mg/L) yields a per capita phosphorus loading of 1.38 g day^{-1} which is slightly lower than the values $1.8\text{-}2 \text{ g day}^{-1}$ reported in the literature for domestic sewage (Alexander and Steven 1976; Palmquist and Hanaeus 2005). The lower value may be achieved because of groundwater infiltration into the sewer network, causing dilution.

Nature of mineral phosphate phases. The elemental composition of about 1340 mineral particles of freeze-dried samples from sewage, biofilm, and sewer sediment, was analyzed by TEM-EDXS. About 40% of these particles were described as phosphate phases. Most of the time, these phosphate minerals are amorphous and do not yield a workable electron diffraction pattern. As illustrated in figure 3, the distribution of Ca/P molar ratios of phosphate particles reveals obvious maximas at Ca/P equal to 0.6, 0.8, 1, 1.27, 1.35, and 1.6. Such atomic ratios likely identify occurrences of hydroxyapatite ($\text{Ca}_{10}(\text{PO}_4)_6(\text{OH})_2$ - Ca/P = 1.6), octacalcium phosphate ($\text{Ca}_8\text{H}_2(\text{PO}_4)_6$ - Ca/P = 1.33), whitlockite ($\text{Ca}_9\text{Mg}(\text{PO}_4)_6(\text{PO}_3\text{OH})$), brushite ($\text{CaHPO}_4 \cdot 2\text{H}_2\text{O}$ - Ca/P = 1), and crandallite ($\text{CaAl}_3(\text{PO}_4)_2$ - Ca/P = 0.6). According to EDX spectra, the Ca/P ratio of 0.8 may be attributed to a Mg-brushite species ($\text{Ca}_{0.8}\text{Mg}_{0.2}\text{HPO}_4 \cdot 2\text{H}_2\text{O}$), whereas the bump around Ca/P = 2.1 may correspond to carbapatite ($\text{Ca}_{10}(\text{PO}_4, \text{CO}_3)_6(\text{OH}, \text{CO}_3)_2$) and/or co-precipitates of apatite and calcium oxalate.

TEM observations are consistent with EDX microanalyses (figure 4). Thus, brushite and Mg-brushite particles typically appear as isolated $0.4\text{-}0.7 \mu\text{m}$ porous spheres (fig. 4a). Brushite usually contains little Mg and S ($\text{Mg}/\text{Ca} < 0.05$ and S/P between 0 and 0.15). Whitlockite and octacalcium phosphate particles (fig. 4b) are both formed by micron-size aggregates, the varying size of subunits (20-100 nm) resulting in granulous structures. Various morphological aspects are found for apatite: in addition to frequent compact aggregates with subunits of about 200 nm (fig. 4c), a hairy-type species (fig. 4d) and a few well crystallized particles were observed (Inset of fig. 4d). Tricalcium phosphate ($\text{Ca}_3(\text{PO}_4)_2$), which also occurs as small aggregates, was rarely identified in the sewer network. Small spheres, $0.2 \mu\text{m}$ in diameter, strongly deficient in calcium ($\text{Ca}/\text{P} \sim 0.5$) were found in biofilms (fig. 4e). They may have been formed in acidic conditions and may correspond to calcium dihydrogen phosphate. However, the O/P ratio of those phases is sometimes close to 2; as reduced inorganic phosphorus has been evidenced in sewage works (Hanrahan et al. 2005 and references herein), it is suspected that phosphite or even hypophosphite calcium species might form within biofilms.

Various aluminum-containing phosphate phases also occur in the sewage. They are tentatively attributed to bearthite ($(\text{Ca}_2\text{Al}(\text{PO}_4)_2(\text{OH}))$ Ca/P = 1, Al/Ca = 0.5) (Fig. 4f), foggite ($(\text{CaAl}(\text{PO}_4)(\text{OH}_2\cdot\text{H}_2\text{O}))$ Ca/P = 1, Al/Ca = 1) (Fig.4g), gatumbaite ($(\text{CaAl}_2(\text{PO}_4)_2(\text{OH})_2\cdot\text{H}_2\text{O})$ Ca/P = 0.5, Al/Ca = 2) (inset of fig. 4h), and crandallite ($(\text{CaAl}_3(\text{PO}_4)_2(\text{OH})_5\cdot\text{H}_2\text{O})$ Ca/P = 0.6, Al/Ca = 3) (fig. 4h). The Al-Ca phosphates do not present a definite morphological aspect and rather appear as either spheres or aggregates similar in size and shape to the previously described calcium phosphate minerals. Their elemental composition frequently comprises S (i.e. SO_4^{2-}) as compensating anion and small amounts of metals such as Fe, Zn, and Pb.

Phosphate species containing iron were rarely found within the sewer network. Single occurrences of strengite ($\text{FePO}_4\cdot 2\text{H}_2\text{O}$), anapaite ($\text{Ca}_2\text{Fe}(\text{PO}_4)_2\cdot 4\text{H}_2\text{O}$), probably melonjosephite ($\text{CaFe}(\text{II})\text{Fe}(\text{III})(\text{PO}_4)_2(\text{OH})$), and even more anecdotic, iron phosphide (Fe_3P) – most likely eroded from cast-iron distribution pipes - were identified in suspended matter, biofilm, and sediment, respectively. Vivianite ($\text{Fe}_3(\text{PO}_4)_2\cdot 8\text{H}_2\text{O}$), a common iron phosphate mineral in freshwater sediments (Nriagu and Dell, 1974; Taylor et al. in press), biological sludges treated with ferrous sulfate (Frossard et al. 1997), and known to control phosphorus availability in septic system plumes (Robertson et al. 1998), was not detected in any of our samples.

Spatial and Temporal evolution of phosphate species in the sewer network. As illustrated in figure 5a, the composition of phosphate minerals slightly evolves along the sewer network. Upstream, the average Ca/P elemental ratio is close to 1.3, the phosphate phases most frequently identified being apatite, octacalcium phosphate, whitlockite, and brushite. Conversely, aluminum-calcium phosphate species are more abundant at downstream sampling sites, while Ca/P ratios decrease to about 0.8. The temporal evolution of Ca/P ratio within suspended matter collected at an upstream sampling site (figure 5b), indicates that the average Ca/P remains close to 1.3 even though soluble phosphate concentration fluctuates markedly during the day. Interestingly, biofilms and sediments taken at a given sampling site, were found to be slightly enriched in hydroxyapatite and calcium-aluminum phosphate phases compared with the associated suspended matter. This suggests that an increased residence time in the sewer network induces a change in phosphate mineralogy.

Chemical extraction results. Typical partitioning of phosphorus among the extracted chemical forms in sewage suspended matter, biofilm, and sediment collected at a given sampling site, is shown in figure 6a. Results are given on the basis of dry weight material after

heating at 550°C for [L-P], [Al-P], [Fe-P], [Ca-P], and on the basis of volatile solid weight (VS) for organic P. Obvious differences between the three types of samples can be observed. Labile P and organic P account for a significant amount of phosphorus in sewage suspended matter, whereas these two geochemical phases are virtually absent in biofilm and sediment. Such results seem consistent with the lower solubility of phosphate carriers identified by TEM-EDXS in the latter samples. The spatial evolution of phosphorus distribution in suspended matter is also in line with TEM-EDXS speciation results (fig. 6b) as aluminum bound phosphate gradually increases downstream. In addition, the amount of P associated with organic matter slightly decreases. However, the P fraction bound to Fe seems disproportionate in comparison with TEM observations. Figure 6b also indicates that P associated with Al is systematically equivalent or higher to the total amount of phosphorus contained in the samples. In fact both [Al-P], [Fe-P], are correlated with [Ca-P] (Fig. 7), which implies a non-specific dissolution of mineral phases during the chemical extraction procedure, and hence, a poor estimate of the actual phosphorus amount associated with the targeted phase.

TEM examination of phosphate species contained in each extracted residue further invalidates the extraction scheme (Table 5). Drastic changes in P chemical forms occur during the water extraction step of labile phosphate: aluminum-calcium phosphates which were not initially present in upstream samples (e.g. crandallite) are found among the residual solids after the water extraction. Similarly, aluminum-containing phosphate phases with small amounts of Fe, are formed upon extraction of organic P. Extraction of [Ca-P] and [Al-P] with NaOH and NaF, respectively, removed all phosphate species except those associated with organic matter. The extraction of P associated with Fe induced the precipitation of iron-calcium phosphate aggregates. Eventually, solely the organic P extraction seemed to respect the initially present calcium-phosphate phases.

The identification of those neoformed species throws serious doubts upon the validity of most sequential extraction schemes used to assess P chemical fractions in presence of amorphous phosphate phases. Poorly-ordered wavellite ($\text{Al}_3(\text{OH})_3(\text{PO}_4)_2 \cdot 5\text{H}_2\text{O}$) was also reported by Frossard et al. (1994) using ^{31}P NMR after HCl extraction of anaerobically-digested and biological sludges. In that case, the authors could not conclude whether wavellite was initially present or precipitated during sequential extraction.

DISCUSSION

Origin of phosphate mineral species. It seems quite trivial to identify biogenic phosphates such as apatite, brushite, octacalcium phosphate, or whitlockite in domestic sewage. Indeed, such phosphate phases are commonly described, though in a pathological context, in human urinary stones (brushite, octacalcium phosphate, whitlockite, carapatite) (Bazin et al. 2007), salivary stones (apatite, brushite, and whitlockite) (Zelentsov et al. 2001), and human guts (brushite) (Gomez-Morilla et al. 2006). However, to our knowledge, such release of micron-size phosphate particles from healthy subjects has not been documented. Chemical modeling of most probable phosphate phases in cow manure suggested the presence of brushite, octacalcium phosphate, β -tricalcium phosphate, and struvite ($\text{MgNH}_4\text{PO}_4 \cdot 6\text{H}_2\text{O}$) (Güngör and Karthikeyan 2005). Likewise, solubility equilibria suggest the formation of hydroxyapatite in urine diluted with tap water, mineral which was indeed identified in samples taken from urine-collecting systems (Udert et al. 2003b). Our own control experiments were consistent with the previous report: SEM examination of particles retained onto a 0.2 μm filter after filtration of fresh human urine, only revealed the presence of well-crystallized calcium oxalate. However, upon a ten-fold dilution in tap water of the same urine samples, small aggregates of hydroxyapatite nanocrystals and ferric-calcium phosphate precipitates of varying composition, were observed. The ferric-calcium aggregates may correspond to the association of phosphate anions with iron oxyhydroxide colloids initially present in tap water. Taking into account these dynamic aspects, it is possible that most phosphate minerals entering the sewer are eventually formed upon dilution of human excretion products by flushing.

The presence of aluminum-calcium phosphate compounds seems more unusual. Until now, bearthite and gatumbaite have only been described in pegmatites, metamorphic rocks, and hydrothermally altered andesites (Duggan et al. 1990; Jambor and Vanko 1993). In contrast, crandallite and foggite have been found in sedimentary environments with physicochemical characteristics comparable to those of the sewer network. Thus, crandallite occurs in coal seams (Ward et al. 1996; Rao and Walsh 1999), in lateritic weathering profiles in which it is formed from the alteration of clay minerals in presence of apatite (Vieillard et al. 1979), or as a secondary precipitate in the presence Al-hydroxides (Schwab et al. 1989). Foggite is also recognized as a secondary mineral in phosphate deposits and seems to result from the decomposition of crandallite (Onac et al. 2002). It is therefore likely that, in the sewer network, those aluminum-calcium phosphate minerals correspond to neofomed phases.

TEM-EDXS observation of these aluminum-containing phosphate species after water-extraction of labile P strongly supports the neofomation hypothesis. In addition, the time

scale associated with the various leaching steps is equivalent to the transit time of sewage within the sewer network.

Phosphate geochemistry in the urban sewer. The variety of phosphate minerals that occur simultaneously in a single sample of sewage, suggests that the thermodynamic equilibrium between phosphate phases and solution is not reached within the sewer system. Thermodynamic non-equilibria are indeed typical of phosphate mineral associations. For instance Nancollas and Tomazic (1974) show that up to four different calcium phosphate phases can be formed in the early stages of precipitation in highly supersaturated solutions seeded with thermodynamically stable hydroxyapatite. Kinetic phenomena are shown to be predominant in controlling the stoichiometry of the species precipitated initially. In our case, the sewage is supersaturated with respect to the more stable phases octacalcium phosphate and hydroxyapatite, but is close to equilibrium with brushite, the most soluble phase (Fig.9)

From a kinetic point of view, this strongly suggests that brushite is formed first, before transforming to apatite and octacalcium phosphate. The hypothesis is supported by the increase in apatite observed between fresh suspended particles and deposited particles (“sediment”) that have had time to age. Along the sewer system, transformation of metastable Ca-phosphate species is further supported by the evolving solution chemistry. If alkaline conditions initially prevail (pH ~ 8.5-9), the pH tends to decrease to about 7.9 at downstream sampling sites. In addition, groundwater infiltrations dilute soluble phosphate contents and increase calcium concentration during sewage transportation (Fig.8a) (Le Bonte et al., in press; Houhou et al. in preparation). These changes may accelerate the formation of octacalcium-phosphate and apatite by partial dissolution of the more soluble species. Interestingly, the characteristic size of the Ca-phosphate phases in the effluent appears to be related to the degree of their supersaturation in solution. The critical nucleation size r^* is related to saturation by the following equation (Wu and Nancollas 1999):

$$r^* = \frac{2\gamma_{SL}\Omega_V}{kT\ln S}$$

where γ_{SL} is the solid-liquid interfacial energy, Ω_V the molecular volume, k the Boltzman's constant, T the temperature, and S the supersaturation. Using γ_{SL} and Ω_V data from Wu and Nancollas (1999), r^* should fall in the range 1-3 nm, 6-174 nm, and 23-110 nm, for brushite, octacalcium phosphate, and apatite, respectively. This is fairly close to the 2-3 nm, 20-100 nm, and 200 nm values frequently determined by TEM. It illustrates the essential role of reaction kinetics on the texture of the mineral phases in the sewer system.

The behaviour of aluminium in the sewer system is more difficult to assess due to less available data. The source of aluminum in the sewer system is not known precisely to date. Dissolved Al is low upstream and increases slightly downstream. Correlation between dissolved Al and dissolved organic carbon in the effluents (Fig. 8b) suggests that Al may be partly complexed to organic ligands. Otherwise, and at first approach, dissolved aluminium should be present as Al-hydroxy ions. Solubility calculations show that the solutions are in equilibrium with a Al-hydroxide phase. Average saturation indices are 0.91 ± 0.06 for amorphous $\text{Al}(\text{OH})_3$, 1.09 ± 0.062 for gibbsite and 1.11 ± 0.063 for diaspore. However no Al-hydroxides have been identified in any particulate fraction of the sewer, and at any collection time. Although close to saturation, Al-hydroxides do not precipitate. This inhibition is most probably explained by complexation of the $\text{Al}(\text{O},\text{OH})_6$ octahedra with phosphate, which blocks the $\text{Al}(\text{O},\text{OH})_6$ polymerisation process. Phosphate ions largely exceed the Al concentration in solution (average $\text{P}/\text{Al} = 400$) in the sewer system. Inhibition or retardation of hydroxide formation by phosphate has been recognized previously (Boisvert et al. 1997) and shown to be effective at P/Al ratios as low as 1.

If Al-hydroxy-phosphate complexes do form in solution, it is straightforward to expect the formation of Al-phosphate minerals. Indeed TEM-EDX analyses confirmed the presence of bearthite, gatumbaite and especially crandallite (Fig. 3). In figure 10 the crandallite solubility curve was plotted against an Al-hydroxy ion. We chose $\text{Al}(\text{OH})_4^-$ as this is one of the dominating species at the pHs encountered in the sewer. The solubility constants used are given in appendix 2. Figure 10 reveals that the sewer solution is undersaturated with respect to crandallite. However the solubility limit is closely approached for pHs below 8.5, which corresponds with the samples from downstream stations, where indeed the mineral has been identified by TEM.

To our knowledge, no solubility constants have yet been determined for minerals such as bearthite or gatumbaite, so that it is not possible to suggest a kinetic sequence for the formation of Al-Ca-phosphates as we did it for the Ca-phosphates. Nonetheless, TEM images show that the morphology of bearthite is alike brushite and crandallite resembles whitlockite or octacalcium phosphate. These similarities suggest that bearthite may form first, and then transform to whitlockite or crandallite.

CONCLUSION

In aquatic systems, phosphorus speciation has often been limited to a simple classification between soluble P and particulate P. This study clearly demonstrates that electron microscopy coupled with EDX spectroscopy provides some useful information on the nature of phosphate amorphous phases that are present in an urban sewer. In particular, this technique reveals the formation of aluminium-calcium phosphate species during sewage transit that could not be detected from particulate P percentages. However, such evolution can not readily be generalized to any sewer system as the ionic content of sewage, and especially the presence of Mg (Nancollas et al. 1976), may strongly alter the observed trend. Nevertheless, a similar study conducted at Levenmouth (Scotland), also showed the presence of foggite, bearthite, gatumbaite, and crandallite at the inlet of the wastewater treatment plant (Lartiges, unpublished results).

Besides a better understanding of the sewer system as a biophysicochemical reactor, the evolution of P speciation incite to better relate the functioning of wastewater treatment plant with the characteristics of the sewer system, especially when a biological phosphate removal is used. Another potential application of P speciation concerns combined sewer overflows and the form of phosphate species exported to the local waterways.

Acknowledgements : This work was mainly funded through a CNRS-INSU (ECODYN) grant which is gratefully acknowledged. Region Lorraine also provided funding through Zone Atelier Moselle. We are grateful to M. Piqué and M. Villeroy (Service hydraulique CUGN) for technical assistance during all field studies. We also wish to thank the staff of SARM (CRPG-UPR 80) where ICP analyses were carried out.

REFERENCES

Alexander G.C., Stevens, R.J. (1976) Per capita phosphorus loading from domestic sewage. *Wat. Res.* 10(9), 757-764.

Bedrock, C.N.; Cheshire, M.V.; Shand, C.A. (1997) The involvement of iron and aluminum in the bonding of phosphorus to soil humic acid. *Commun. Soil. Sci. Plant Anal.* 28, 961-971.

Boisvert, J.P., To, T.C., Berrak, A., Jolicoeur, C., (1997) Phosphate adsorption in flocculation processes of aluminum sulphate and poly-aluminium-silicate-sulphate. *Wat. Res.* 31, 1939-1946.

Butler, D., Fnedier, E., Gatt, K. (1995) Characterising the quantity and quality of domestic wastewater inflows. *Wat. Sci. Technol.* 31(7), 13-24.

Duggan, M.B., Jones, M.T., Richards, D.N.G., Kamprad, J.L. (1990) Phosphate minerals in altered andesite from Mount Perry, Queensland, Australia. *Can. Mineral.* 28, 125-131.

Carignan, J., Hild, P., Mevelle, G., Morel, J., Yeghicheyan, D. (2001) Routine analysis of trace elements in geological samples using flow injection and low pressure on-line liquid chromatography coupled to ICP-MS: a study of geochemical reference materials BR, DR-N, UB-N, AN-G, and GH. *Geostandards Newsletter* 25, 187-198.

Chang, S.G., Jackson, M.L. (1957) Fractionation of soil phosphorus. *Soil. Sci.* 84, 133-144.

Chen, G.H., Leung, D.H.W., Hung, J.C. (2001) Removal of dissolved organic carbon in sanitary gravity sewer. *J. Environ. Eng.* 127, 1-7.

Crabtree, R.W. (1989) Sediments in sewers. *J. Inst. Water Environ. Manag.*, 3(3), 569-578.

Eggers, E. (1986) Full-scale experiences with phosphate crystallisation in a crystalreactor. *Wat. Sci. Tech.* 23, 819-824.

El Samrani, A.G., Lartiges, B.S., Ghanbaja, J., Yvon, J., Kohler, A. (2004) Trace element carriers in combined sewer during dry and wet weather: an electron microscope investigation. *Wat. Res.* 38, 2063-2076.

Froelich, P.N. Kinetic control of dissolved phosphate in natural rivers and estuaries: a primer on the phosphate buffer mechanism. *Limnol. Oceanogr.* 33(4) 649-668.

Frossard, E., Tekely, P., Grimal, J.Y. (1994) Characterization of phosphate species in urban sewage sludges by high-resolution solid-state ³¹P NMR. *Eur. J. Soil Sci.* 45, 403-408.

Frossard, E., Bauer, J.P., Lothe, F. (1997) Evidence of vivianite in FeSO₄-flocculated sludges. *Wat. Res.* 31(10), 2429-2454.

Gaboreau, S., Vieillard, P. (2004) Prediction of Gibbs free energies of formation of minerals of the alunite supergroup. *Geochim. Cosmochim. Acta* 68, 3307-3316

Gomez-Morilla, I., Thoree, V., Powell, J.J., Kirkby, K.J., Grime, G.W. (2006) Identification and quantitative analysis of calcium phosphate microparticles in intestinal tissue by nuclear microscopy. *Nucl. Instr. and Meth. B* 249, 665-669.

Guisasola, A., de Haas, D., Keller, J., Yuan, Z. (2008) Methane formation in sewer systems. *Wat. Res.* 42, 1421-1430.

Güngör, K., Karthikeyan, K.G. (2005) Probable phosphorus solid phases and their stability in anaerobically digested dairy manure. *Trans. ASABE* 48(4), 1509-1520.

Halliwell, D.J., McKelvie, I.D., Hart, B.T., Dunhill, R.H. (2001) Hydrolysis of triphosphate from detergents in a rural waste water system. *Wat. Res.* 35(2), 448-454.

Hanrahan, G., Salmassi, T.M., Khachikian, C.S., Foster, K.L. (2005) Reduced inorganic phosphorus in the natural environment: significance, speciation and determination. *Talanta* 66, 435-444.

Hvitved-Jacobsen, T., Raunkjaer, K., Nielsen, P.H. (1995) Volatile fatty acids and sulfide in pressure mains. *Wat. Sci. Tech.* 31(7), 169-179.

Houhou, J., Lartiges, B.S., France-Lanord, C., Poix, S. (in preparation) Identification of water sources in an urban sewer using multiple isotopic tracers.

Jambor, J.L., Vanko, D.A. (1993) New mineral names. *Am. Mineral.* 78, 1314-1319.

Jolley, D., Maher, W., Cullen, P. (1998) Rapid method for separating and quantifying orthophosphate and polyphosphates: application to sewage samples. *Wat. Res.* 32(3) 711-716.

Keizer, M.G., Van Riemsdijk, W.H. (1998) ECOSAT. Department Environmental Sciences, Sub department Soil Sciences and Plant Nutrition, Wageningen University. Version 4.7, 76 p.

Kittrick, J.A. (1966) *Soil. Sci. Soc. Am. Proc.* 30, 595-698.

Le Bonté, S., Pons, M.N., Potier, O., Rocklin, P. Relation between conductivity and ion content in urban wastewater. *Revue des Sciences de l'Eau* (in press).

Lindsay, W.L. (1979) *Chemical equilibria in soils*. Wiley Interscience New York, 449p.

McKelvie, I.D. (2005) Separation, preconcentration and speciation of organic phosphorus in environmental samples. In *Organic Phosphorus in the Environment*; Turner, B.L., Frossard, E., Bladwin, D.S., Eds; CAB International: Wallingford, 2005; pp 1-20.

Mesmer, R.E, Base, C.F. Jr. (1974) *J. Soln. Chem.* 3, 307-321.

Moreau, S (1997) Investigation of Vilaine watershed. PhD thesis, Rennes I University.

Mulkerrins, D., Dobson, A.D.W., Colleran, E. (2004) Parameters affecting biological phosphate removal from wastewaters. *Environment International* 30, 249-259.

Murphy, J., Riley, J.P. A modified single solution method for the determination of phosphate in natural waters. *Anal. Chim. Acta* 1962, 27, 31-36.

Nancollas, G.H., Tomazic, B. (1974) Growth of calcium phosphate on hydroxyapatite crystals. Effect of supersaturation and ionic medium. *J. Phys. Chem.* 78(22), 2218-2224.

Nancollas, G.H., Tomazic, B., Tomson, M. (1976) The precipitation of calcium phosphates in presence of magnesium. *Croat. Chem. Acta* 48, 431-438.

Nriagu, J.O., Dell, C.I. (1974) Diagenetic formation of iron phosphates in recent lake sediments. *Am. Min.* 59, 934-946.

Nriagu, J.O. (1976) Phosphate-clay mineral relations in soils and sediments. *Canadian J. Earth Sci.* 13, p.717.

Onac, B.P. Breban, R., Kearns, J., Tamas, T. (2002) Unusual minerals related to phosphate deposits in Cioclovina Cave, Sureanu Mts (Romania). *Theoretical and Appl. Karst.* 15, 27-34.

Owens, P.N., Walling, D.E. (2002) The phosphorus content of fluvial sediment in rural and industrialized river basins. *Wat. Res.* 36, 685-701.

Palmquist, H., Hanaeus, J. (2005) Hazardous substances in separately collected grey- and blackwater from ordinary Swedish households. *Sci. Total Env.* 348, 151-163.

Raunkjaer, K., Hvitved-Jacobsen, T., Nielsen, P.H. (1995) Transformation of organic matter in a gravity sewer. *Wat. Environ. Res.* 67(2), 181-188.

Rao, P.D., Walsh, D.E. (1999) Influence of environments of coal deposition on phosphorous accumulation in a high latitude, northern Alaska, coal seam. *Int. J. Coal Geol.* 38, 261-284.

Robertson, W.D., Schiff, S.L., Ptacek, C.J. (1998) Review of phosphate mobility and persistence in 10 septic system plumes. *Ground Wat.* 36, 1000-1010.

Schwab, R.G., Herold, H., Da Costa, M.L., De Oliveira, N.P. (1989) The formation of aluminous phosphates through lateritic weathering of rocks. *Weathering.* 2, 369-386.

Schwab, R.G., Götz, C., Herold, H., De Oliveira, N.P. (1993) Compounds of the crandallite type: Thermodynamic properties of Ca-, Sr-, Ba-, Pb-, La-, Ce-, to Gd-phosphates and -arsenates. *N. Jb. Miner. Mh.* 12, 551-568.

Shock, E.L., Helgeson, H.C. (1988) Calculation of the thermodynamic properties and transport properties of aqueous species and equation of state predictions to 5kb and 1000°C. *Geochim. Cosmochim. Acta* 52, 2009-2036.

Robie, R.A., Hemingway, B.S. (1995) Thermodynamic properties of minerals and related substances at 298.15 K and 1bar (10^5 pascals) pressure and higher temperatures. *Bulletin 2131 U.S. Geological Survey.* Taylor, K.G., Boulton, S. (2007) The role of grain dissolution and diagenetic mineral precipitation in the cycling of metals and phosphorus: A study of a contaminated urban freshwater sediment. *Appl. Geochem.* 22, 1344-1358.

Taylor, K.G., Hudson-Edwards, K.A., Bennett, A.J., Vishnyakov, V. (in press) Early diagenetic vivianite [$\text{Fe}_3(\text{PO}_4)_2 \cdot 8\text{H}_2\text{O}$] in a contaminated freshwater sediment and insights into zinc uptake: a μ -EXAFS, μ -XANES and Raman study. *Appl. Geoch.*

Tchobanoglous, G., Burton, F.L., Stensel, H.D. (2003) *Wastewater Engineering. Treatment and Reuse.* 4th ed. (Int. Ed). Metcalf and Eddy, McGraw-Hill, New York, 181-191.

Udert, K.M., Larsen, T.A., Biebow, M., Gujer, W. (2003a) Precipitation dynamics in a urine-collecting system. *Wat. Res.* 37(11), 2571-2582.

Udert, K.M., Larsen, T.A., Gujer, W. (2003b) Estimating the precipitation potential in urine-collecting systems. *Wat. Res.* 37, 2667-2677.

Vieillard, P., Tardy, Y., Nahon, D. (1979) Stability fields of clays and aluminum phosphates: parageneses in lateritic weathering of argillaceous phosphatic sediments. *Am. Mineral.* 64, 626-634.

Ward, C.R., Corcoran, J.F., Saxby, J.D., Read, H.W. (1996) Occurrence of phosphorus minerals in Australian coal seams. *Int. J. Coal Geol.* 30, 185-210.

Warith, M.A., Kennedy, K., Reitsma, R. (1998) Use of sanitary sewer as wastewater pre-treatment systems. *Waste Manag.* 18, 235-247.

Wu, W., Nancollas, G.H. (1999) Determination of interfacial tension from crystallisation and dissolution data: a comparison with other methods. *Adv. Colloid Interface Sci.* 79, 229-279.

Yongsiri, C., Vollertsen, J., Hvitved-Jacobsen, T. (2004) Hydrogen sulfide emission in sewer networks: a two-phase modeling approach to the sulfide cycle. *Wat. Sci. Technol.* 50(4), 161-168.

Zelentsov, E.L., Moroz, T.N., Kolmogorov, Y.P., Tolmachev, V.E., Dragun, G.N., Palchik, N.A., Grigorieva, T.N. (2001) The elemental SRXRF analysis and mineral composition of human salivary stones. *Nucl. Instr. and Meth. A* 470, 417-421.

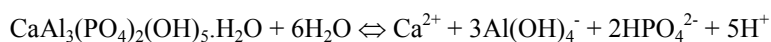
Appendix 1:

Ca-phosphate Solubility constants (25 °C, 1 atm) (Lindsay, 1979)

Mineral phase / reaction	K°
Octacalciumphosphate: $\text{Ca}_4\text{H}(\text{PO}_4)_3 \cdot 2.5\text{H}_2\text{O} \Leftrightarrow 4\text{Ca}^{2+} + 2.5\text{H}_2\text{O} + 3\text{HPO}_4^{2-}$	-9.84
Brushite $\text{CaHPO}_4 \cdot 2\text{H}_2\text{O} + \text{H}^+ \Leftrightarrow \text{Ca}^{2+} + \text{H}^+ + \text{HPO}_4^{2-} + 2\text{H}_2\text{O}$	-6.57
Hydroxyapatite $\text{Ca}_5(\text{PO}_4)_3\text{OH} + 4\text{H}^+ \Leftrightarrow 5\text{Ca}^{2+} + 3\text{HPO}_4^{2-} + \text{H}_2\text{O}$	-7.14
β -tricalciumphosphate (whitlockite) $\text{Ca}_3(\text{PO}_4)_2 + 2\text{H}^+ \Leftrightarrow 3\text{Ca}^{2+} + 2\text{HPO}_4^{2-}$	-4.22
Crandallite $\text{CaAl}_3(\text{PO}_4)_2(\text{OH})_5 \cdot \text{H}_2\text{O} + 7\text{H}^+ \Leftrightarrow \text{Ca}^{2+} + 3\text{Al}^{3+} + 2\text{HPO}_4^{2-} + 6\text{H}_2\text{O}$	1.5
Al(OH) ₃ amorphous $\text{Al}(\text{OH})_3 + 3\text{H}^+ \Leftrightarrow \text{Al}^{3+} + 3\text{H}_2\text{O}$	9.66
Gibbsite $\text{Al}(\text{OH})_3 + 3\text{H}^+ \Leftrightarrow \text{Al}^{3+} + 3\text{H}_2\text{O}$	8.04
Diaspore $\text{Al}(\text{OH})_3 + 3\text{H}^+ \Leftrightarrow \text{Al}^{3+} + 3\text{H}_2\text{O}$	7.92

Appendix 2

The solubility constant of crandallite was calculated for the reaction:



using ΔG°_f values listed below. Log(K) values vary from -63 to -69 when alternate ΔG°_f values for $\text{Al}(\text{OH})_4^-$, HPO_4^{2-} and crandallite are used.

SPECIES	ΔG°_f (kJ/mol)	REFERENCE
Ca^{2+}	-552.79	1
$\text{Al}(\text{OH})_4^-$	-1307.33 -1305.4	2 3
HPO_4^{2-}	-1097.07 -1089.3	4 3
$\text{H}_2\text{O liq}$	-237.18	5

crandallite	-5608.64	6
	-5596.5	7
	-5618.69	8

1. Shock and Helgeson (1988) cited in Gaboreau and Vieillard (1993), 2. Kittrick (1966) cited in Lindsay (1979), 3. Michard xxx, 4. Mesmer and Base (1974) cited in Lindsay (1979), 5. Robie and Hemingway (1995) cited in Gaboreau and Vieillard (1993), 6. Schwab et al. (1989), 7. Vieillard et al. (1979) cited in Schwab et al. (1989), 8. Nriagu (1976) cited in Schwab et al. (1989).